1999

Nanometer-Scale Probing of Potential-Dependent Electrostatic Forces, Adhesion, and Interfacial Friction at the Electrode/Electrolyte Interface

Shane D. Campbell, *University of Virginia - Main Campus*
Andrew C. Hillier, *University of Virginia - Main Campus*

Nanometer-Scale Probing of Potential-Dependent Electrostatic Forces, Adhesion, and Interfacial Friction at the Electrode/Electrolyte Interface

Shane D. Campbell and Andrew C. Hillier*

Department of Chemical Engineering and Center for Electrochemical Science and Engineering, University of Virginia, Charlottesville, Virginia 22903-2442

Received September 1, 1998. In Final Form: November 30, 1998

The atomic force microscope (AFM) was used to examine the influence of an applied electrochemical potential on the interfacial properties of the electrode/electrolyte interface. Measurements of electrostatic force, adhesion, and friction coefficient were performed at two different electrode surfaces: glassy carbon and a thin film of sulfonate-derivatized poly(aniline) (SPANi). At the carbon electrode, changes in electrostatic force between probe and substrate exhibited a potential-dependent transition from repulsive to attractive values at potentials negative and positive of the potential of zero charge (E_{pzc}). Simultaneous measurements of tip−substrate adhesion and friction coefficient showed a change from low to high values over the same potential range, suggesting a common mechanism dominated by the electrostatic force. Measurement of these same properties at a SPANi-coated electrode also displayed a potential-dependent response. The electrostatic force and the adhesion tracked with the oxidation state of the initially neutral film. However, the friction coefficient appeared insensitive to the charge state of the polymer. A calculation of the forces between probe and substrate using DLVO theory accurately reflected the measured force curves as well as the change in adhesive force as a function of surface charge. Consideration of the forces that determine the friction coefficient suggested that the influence of electrostatic interactions was strongly dependent upon the geometry of the tip−sample contact and the presence of microgaps between the tip and the substrate over which electrostatic forces could operate. The absence of potential-dependent friction at the SPANi/electrolyte interface reflected a compliant substrate, which gave rise to a predominantly adhesive tip/sample contact.

Introduction

The development of scanning probe microscopy, including scanning tunneling microscopy (STM),[1] atomic force microscopy (AFM),[2,3] and scanning electrochemical microscopy (SECM),[4−6] and its application in electrochemical systems has significantly advanced our understanding of the microscopic surface phenomena associated with electrochemical events. These techniques have proven highly valuable in characterizing electrochemical systems because of their ability to provide in-situ and real-time images of electrode surfaces while under electrochemical control with a resolution ranging from microns to angstroms. A wide variety of electrochemical systems have been explored with these techniques, ranging from simple adsorption and ion exchange to electrodeposition and corrosion.[7]

The ability of scanning probe methods to perform interfacial property measurements, in addition to topographical imaging, adds the capability of connecting structure with function at high spatial resolution and poses the potential to considerably advance our ability to understand and control the properties of interfaces at a microscopic level. An impressive array of surface-sensitive characterization techniques based upon the scanning probe have been developed that now provide access to chemistry,[8] temperature,[9] elasticity,[10] surface forces,[11] friction,[12] and many other interfacial properties.

The ability of atomic force microscopy to measure surface forces has been demonstrated in an ever increasing number of colloidal, polymer, biological, and electrochemical systems.[13] This application in electrochemical environments provides a unique view of the electrostatic double layer and related charge-transfer processes that can be used to quantifiably measure surface charge[14−17] and also to image electrostatic domains at nanometer resolution.[18,19]

Adhesive forces have been examined in electrochemical systems and reflect changes in the surface properties of

* To whom correspondence should be addressed.

(1) Binnig, G.; Rohrer, H.; Gerber, C.; Weibel, E. *Phys. Rev. Lett.* **1982**, *49*, 57.
(2) Binnig, G.; Quate, C. F.; Gerber, C. *Phys. Rev. Lett.* **1986**, *56*, 930.
(3) Binnig, G.; Gerber, C.; Stoll, E.; Albrecht, R.; Quate, C. *Europhys. Lett.* **1987**, *3*, 1281.
(4) Kwak, J.; Bard, A. J. *Anal. Chem.* **1989**, *61*, 1794.
(5) Bard, A. J.; Fan, F.-R. F.; Pierce, D. T.; Unwin, P. R.; Wipf, D. O.; Zhou, F. *Science* **1991**, *254*, 68−74.
(6) Bard, A. J.; Cliffel, D. E.; Demaille, C.; Fan, F. R. F.; Tsionsky, M. *Ann. Chim.* **1997**, *87*, 15−31.
(7) Gewirth, A. A.; Niece, B. K. *Chem. Rev.* **1997**, *97*, 1129−1162.
(8) Frisbie, C. D.; Rozsnyai, L. F.; Noy, A.; Wrighton, M. S.; Lieber, C. M. *Science* **1994**, *265*, 2071.
(9) Majmumdar, A.; Lai, J.; Chandrachood, M.; Nakabeppu, O.; Wu, Y.; Shi, Z. *Rev. Sci. Instrum.* **1995**, *66*, 3584.
(10) Heuberger, M.; Dietler, G.; Schlapbach, L. *Nanotechnology* **1995**, *6*, 12−23.
(11) Ducker, W. A.; Senden, T. J.; Pashley, R. M. *Langmuir* **1992**, *8*, 1831−1836.
(12) Carpick, R. W.; Salmeron, M. *Chem. Rev.* **1997**, *97*, 1163−1194.
(13) Butt, H.-J.; Jaschke, M.; Ducker, W. *Bioelectrochem. Bioenerg.* **1995**, *38*, 191−201.
(14) Raiteri, R.; Grattarola, M.; Butt, H. J. *J. Phys. Chem.* **1996**, *100*, 16700−16705.
(15) Raiteri, R.; Preuss, M.; Grattarola, M.; Butt, H. J. *Colloids Surf., A* **1998**, *136*, 191−197.
(16) Hillier, A. C.; Kim, S.; Bard, A. J. *J. Phys. Chem.* **1996**, *100*, 18808−18817.
(17) Hu, K.; Fan, F. R. F.; Bard, A. J.; Hillier, A. C. *J. Phys. Chem. B* **1997**, *101*, 8298−8303.
(18) Manne, S.; Cleveland, J. P.; Gaub, H. E.; Stucky, G. D.; Hansma, P. K. *Langmuir* **1994**, *10*, 4409.
(19) Aksay, I. A.; Trau, M.; Manne, S.; Honma, I.; Yao, N.; Zhou, L.; Fenter, P.; Eisenberger, P. M.; Gruner, S. M. *Science* **1996**, *273*, 892.

10.1021/la981137u CCC: $18.00
Published on Web 01/09/1999

electrodes. Adhesive force measurements between Si_3N_4 and gold showed a strong increase at potentials where hydrogen bonding could occur between the tip and the substrate.[20] Potential-dependent adhesive force measurements between ferrocene-terminated alkanethiolate monolayers showed a titration-like response that was attributed to a change in surface tension between reduced and oxidized states.[21] Measurements of the adhesion between two electrodes functionalized with poly(vinylferrocene) films also showed a potential-dependent switching of the adhesive force.[22]

The friction coefficient has also been examined at electrode surfaces. Early applications of polaromicrotribometry, which involved the simultaneous measurement of surface friction and electrochemistry, indicated that friction and wear at metal and metal oxide interfaces varied with electrode potential.[23,24] The potential dependence of the friction coefficient between a platinum slider and wire showed a parabolic dependence that exhibited a maximum at the potential of zero charge.[25] A recent AFM study of the friction force at graphitic steps showed a variation with electrode potential that suggested an electrostatic component dominated this process.[26]

Friction coefficients have been observed to vary with adsorption-induced surface charges. For example, pH-dependent variations in friction have been observed in several systems. The friction coefficient between metal oxides in aqueous solutions varied with surface charge, as controlled by the solution pH, for low applied loads.[27] At high applied loads, it was suggested that the friction coefficient was independent of surface charge. Friction and adhesion measurements between surfaces functionalized with self-assembled monolayers containing various chemical function groups were shown to exhibit variations attributed to the charge state of ionizable groups.[28,29] Friction coefficients between Si_3N_4 and SiO_2 surfaces were also shown to vary with pH in electrolyte solutions according to changes in surface charge near the isoelectric point.[30]

Our goal in this work was to apply a combination of interfacial property measurements available with atomic force microscopy in order to characterize electrochemically induced changes at the electrode/electrolyte interface. In this report, we examine the interfaces of two different electrode surfaces, glassy carbon and a sulfonated poly(aniline) (SPANi), in an aqueous electrolyte solution as a function of the applied electrochemical potential. Specifically, we use atomic force microscopy to simultaneously measure surface forces, adhesion, and the friction coefficient at an electrode surface as the electrochemical potential is varied. Experimental results are compared to calculations of the interfacial forces using DLVO theory, and a mechanism for the observed variations in these properties is proposed.

Experimental Section

Materials. *(a) Reagents.* Aqueous solutions of KCl were prepared from reagent grade chemicals (Aldrich) in 18 MW deionized water (Milli-Q Plus, Millipore Corp), and pH values were adjusted to a constant value (± 0.5) by adding 0.01 M KOH or 0.01 M HCl and monitored by a Fisher-Scientific Accumet pH meter (Fisher Scientific). Immediately prior to use, the solutions were deaerated with nitrogen for 15 min.

(b) Synthesis of Sulfonated Poly(aniline). Poly(aniline) (PANi) was synthesized following the procedure of Barthet and Guglielmi.[31] Sulfonation of PANi to create the self-doped form (SPANi) was achieved following the substitution method of Yue and Epstein.[32,33]

(c) Substrate Preparation. Glassy carbon electrode substrates (Goodfellow Metals) were prepared by press-fitting a 12 mm diameter glassy carbon disk into Teflon. The electrode surface was polished to optical smoothness using successively finer grades of diamond and silica paste (15, 6, 3, 1, 0.3, and 0.05 mm; Buehler, Lake Bluff, IL). The electrochemically active area was 0.6 cm^2, and atomic force microscopy showed a surface having a root-mean-square roughness of 2.1 nm/μm^2 with a maximum peak-to-valley height of 4.4 nm over a 1 μm × 1 μm area. Prior to use, the substrate was sonicated for 15 min to remove any polishing particles. The electrode was then rinsed in ethanol and copious amounts of purified water and blown dry under nitrogen.

SPANi-coated electrodes were prepared by dissolving approximately 100 mg of the purple/black solid in 20 mL of 0.1 M NH_4OH to make a light-blue solution. A 100 μL droplet was placed on a carbon substrate and allowed to dry in a desiccator cabinet. Solvent evaporation was accompanied by the evolution of NH_3 gas, which left a shiny, green film on the electrode surface. AFM imaging of the dried polymer depicted a uniform structure having a roughness of 4.2 nm/μm^2 with a maximum peak-to-valley height of 10 nm over a 1 μm × 1 μm area.

(d) Probe Preparation. Force curves were acquired using a microfabricated AFM cantilever that had been functionalized with a silica sphere in a fashion similar to the procedure of Ducker, Senden, and Pashley.[11] A silica sphere with a nominal diameter of 10−20 μm (Polysciences) was attached to the tip of a commercially available AFM cantilever (Nanoprobe, Park Scientific) using thermal-setting epoxy resin (Epon 1002, Shell) and an optical microscope with a three-dimensional positioning stage (Epiphot, Nikon). Immediately prior to use, the tip was rinsed with ethanol, rinsed with purified water, and blown dry with nitrogen.

Methods. *(a) Equipment.* Force, friction, and adhesion measurements were performed with a Molecular Imaging scanning probe microscope (Molecular Imaging, Inc.) controlled with a Nanoscope E controller (Digital Instruments).

(b) Electrochemistry. Experiments were carried out in a Teflon "open-cup" style fluid cell. A three-electrode design was used for electrochemical measurements with the substrate of interest serving as the working electrode, a Pt counter electrode (CE), and a Ag quasi-reference electrode (AgQRE). All electrode potentials are cited with respect to this AgQRE reference. Electrochemical control of the cell was effected with a Molecular Imaging PicoStat (Molecular Imaging, Inc.) under computer control.

(c) Force and Adhesion Measurements. Calibration of the cantilever deflection was achieved by measuring the slope of the photodiode detector voltage while the tip was in contact with the substrate in the constant-compliance region of the force curve. This voltage was converted to a distance in nanometers using the piezoelectric scanner's *z*-calibration. The *z*-calibration of the scanner was verified using the optical interference effect described by Jaschke and Butt.[34] The cantilever's normal spring constant

(20) Serafin, J. M.; Gewirth, A. A. *J. Phys. Chem. B* **1997**, *101*, 10833−10838.
(21) Green, J. B. D.; McDermott, M. T.; Porter, M. D. *J. Phys. Chem.* **1996**, *100*, 13342−13345.
(22) Hudson, J. E.; Abruna, H. D. *J. Am. Chem. Soc.* **1996**, *118*, 6303.
(23) Bruno, F.; Dubois, J. E. *Electrochim. Acta* **1972**, *17*, 1161−1170.
(24) Dubois, J. E.; Lacaze, P. C.; Courtel, R.; Herrmann, C. C.; Maugis, D. *J. Electrochem. Soc.* **1975**, *122*, 1454−1460.
(25) Bockris, J. O. M.; Argade, S. D. *J. Chem. Phys.* **1968**, *50*, 1622−1623.
(26) Weilandt, E.; Menck, A.; Binggeli, M.; Marti, O. In *Nanoscale Probes of the Solid/Liquid Interface*; Gewirth, A. A., Siegenthaler, H., Eds.; Kluwer Academic Publishers: Dordrecht, The Netherlands, 1995; pp 307−315.
(27) Kelsall, G. H.; Zhu, Y.; Spikes, H. A. *J. Chem. Soc., Faraday Trans.* **1993**, *89*, 267−272.
(28) Noy, A.; Frisbie, C. D.; Rozsnyai, L. F.; Wrighton, M. S.; Lieber, C. M. *J. Am. Chem. Soc.* **1995**, *117*, 7943−7951.
(29) Vezenov, D. V.; Noy, A.; Rozsnyai, L. F.; Lieber, C. M. *J. Am. Chem. Soc.* **1997**, *119*, 2006−2015.
(30) Marti, A.; Hahner, G.; Spencer, N. D. *Langmuir* **1995**, *11*, 4632−4635.
(31) Barthet, C.; Guglielmi, M. *J. Electroanal. Chem.* **1995**, *388*, 35.
(32) Yue, J.; Epstein, A. J. *J. Am. Chem. Soc.* **1990**, *112*, 2800.
(33) Yue, J.; Wang, A.; Cromack, K. R.; Epstein, A. J.; MacDiarmid, A. G. *J. Am. Chem. Soc.* **1991**, *113*, 2665.
(34) Jaschke, M.; Butt, H.-J. *Rev. Sci. Instrum.* **1995**, *66*, 1258.

k_N was determined using the procedure of Cleveland,[35] where a series of end masses were added to the tip and the change in the cantilever's resonance frequency was recorded. This method provided a normal spring constant of $k_N = 0.65 \pm 0.12$ N m^{-1} for the cantilevers used here.

Surface force measurements were acquired during an approach/retract cycle, where the tip was brought into contact with the sample by scanning approximately 250 nm toward and away from the sample. Adhesion or pull-off force measurements were achieved by analyzing the retract portion of a force curve. The pull-off force was determined as the magnitude of the tip force required to separate the tip from the sample. To facilitate data acquisition and improve the accuracy of the measured adhesion force, a series of 256 force curves was acquired at each potential value using the Force-Volume operational mode available in the Nanoscope controller software (Digital Instruments). The resulting array of force curves was imported into the Igor Pro data analysis program (Wavemetrics) and analyzed using a custom calculation macro. The value reported for the pull-off force at each potential represents the average value of the 256 curves, and the error bars represent the standard deviation of these data.

(d) Friction Measurements. The lateral force between the tip and substrate was determined by recording the lateral tip excursion as given by the voltage difference generated between lateral photodiode sections during cantilever twisting. All data were recorded with the tip scanning perpendicular to the cantilever's long axis. The lateral spring constant was estimated using the ratio of lateral to normal spring constants, which gave a value of $k_L = 255$ N m^{-1}.[28] Calibration of the lateral tip deflection in the photodiode detector was achieved by measuring the slope of the initial sticking region of a lateral force trace at a mica substrate in deionized water according to the procedure of Liu, Wu, and Evans.[36] However, the accuracy of this calibration method has recently come under question.[37,38] It has been suggested that this calibration method provides a measure of the *stiffness* of the tip/sample interface, which includes contributions from the lateral stiffness of the tip, the cantilever, and the substrate.

The friction coefficient (μ) was determined by disabling the slow scan axis and capturing a friction loop, which is a trace of the lateral force, while the tip was scanned approximately 100 nm in the fast scan direction.[36,39] The magnitude of the lateral force was determined by taking the average of the forward and reverse scans. The friction coefficient was determined by plotting the lateral force as a function of the applied normal load, with the slope corresponding to the friction coefficient. Friction coefficient measurements were performed over a range of applied electrochemical potentials by simply repeating this procedure at different potential values.

Results and Discussion

The two electrode materials examined in this work include glassy carbon and sulfonate-derivatized poly(aniline) (SPANi, **1**).[32,33] Under the conditions reported

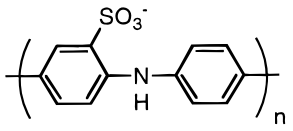

1

here, changing the electrochemical potential applied at the carbon surface results in simple double-layer charging without adsorption or charge-transfer reactions. In contrast, electrochemical cycling of SPANi leads to polymer oxidation or reduction.

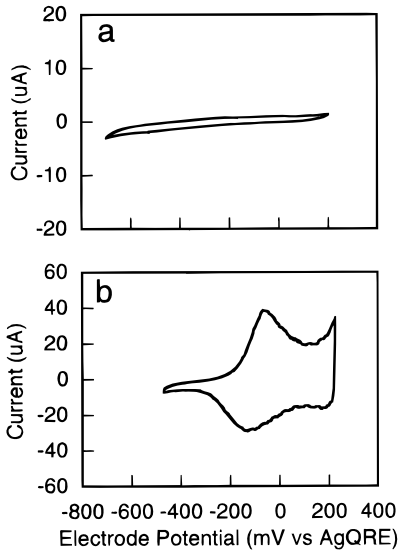

Figure 1. Cyclic voltammetry of (a) glassy carbon and (b) sulfonated poly(aniline) electrodes taken in 1 mM KCl solution. The solution pH values were adjusted to 5.2 (±0.5) and 2.5 (±0.5) for parts a and b, respectively. Electrode potentials are cited with respect to the silver quasi-reference electrode (AgQRE). The electrode areas were each approximately 0.6 cm^2, and the scan rate was 20 mV/s.

Electrochemistry. Figure 1 shows the results of cyclic voltammetric measurements performed on glassy carbon and SPANi-coated electrodes. The response of the glassy carbon electrode, in a 1 mM KCl solution at pH = 5.2, suggests a clean, nonreactive surface. The absence of current peaks over the range from −700 to +200 mV illustrates the absence of charge-transfer and adsorption processes. Thus, excursions in electrochemical potential simply act to charge the electrode between negative and positive values. In contrast, an electrode coated with SPANi exhibits a response characteristic of polymer oxidation/reduction. Oxidation occurs with a current peak at approximately −100 mV. However, this potential value is highly dependent on both the solution pH and the salt concentration due to ion and proton exchange in the polymer.[33] The relatively large capacitive current observed following oxidation reflects a transition to the conducting form of the polymer. SPANi possesses a net negative charge when in the reduced state due to the presence of the sulfonate groups. Following oxidation, SPANi obtains a nominally neutral or positive charge, depending upon the sulfonate content and the degree of polymer oxidation. A purely neutral oxidized state would require the degree of oxidation to be equal to the sulfonate content.

Surface Forces. Measurement of the forces between a SiO_2 tip and the carbon and SPANi substrates was performed at specific electrode potentials over the range of values shown in Figure 1. In each case, the electrode potential was initially held at a negative value and then slowly increased toward more positive values. The forces measured between SiO_2 and glassy carbon in aqueous solution containing 1 mM KCl and pH = 5.2 varied with the electrochemical potential applied to the substrate. At pH = 5.2, SiO_2 possesses a negative surface charge with a surface potential of approximately −41 mV.[16] At negative potential values, the substrate electrode is also negatively charged. The interaction forces measured between probe and substrate (Figure 2a) under these conditions displayed

(35) Cleveland, J. P.; Manne, S.; Bocek, D.; Hansma, P. K. *Rev. Sci. Instrum.* **1993**, *64*, 403.
(36) Liu, Y.; Wu, T.; Evans, D. F. *Langmuir* **1994**, *10*, 2241−2245.
(37) Lantz, M. A.; O'shea, S. J.; Hoole, A. C. F.; Welland, M. E. *Appl. Phys. Lett.* **1997**, *70*, 970−972.
(38) Carpick, R. W.; Ogletree, D. F.; Salmeron, M. *Appl. Phys. Lett.* **1997**, *70*, 1548−1550.
(39) Liu, Y. H.; Evans, D. F.; Song, Q.; Grainger, D. W. *Langmuir* **1996**, *12*, 1235−1244.

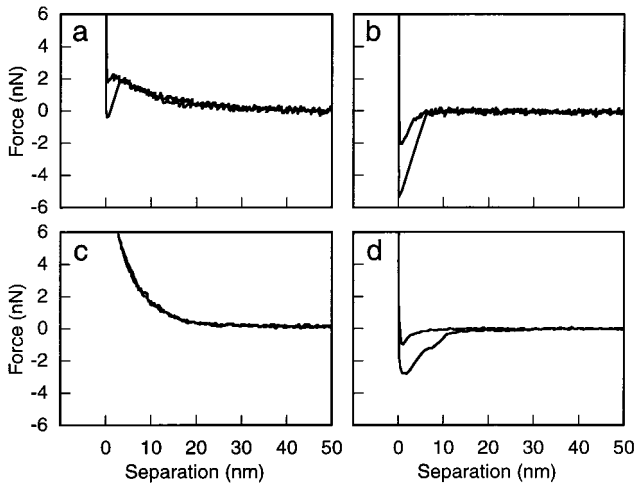

Figure 2. Representative force curves between the tip and substrate under potential control. Forces between the SiO_2 tip and the glassy carbon disk in an aqueous solution of 1 mM KCl at 25 °C and pH = 5.2 at applied potentials of (a) −500 mV and (b) +100 mV (vs AgQRE). Forces between the SiO_2 tip and the sulfonated poly(aniline) SPANi-coated electrode in 1 mM KCl at 25 °C and pH = 2.5 at applied potentials of (c) −350 mV and (d) +250 mV (vs AgQRE). The hysteresis between the approach curve and the retract curve in these data illustrates the pull-off force. Each curve portrays a representative force curve at the specified electrode potential.

a repulsive interaction as the tip−sample separation reduced below 30 nm. The long-range repulsion is due to electrostatic forces while the short-range attraction and the snap-to-contact seen at separations below 5 nm reflect the onset of attractive van der Waals interactions. Hysteresis between approach and retract curves shows a significant pull-off force ($F_{pull-off}$), which indicates adhesive interactions between the tip and the substrate (vide infra).

As the electrode potential is increased to more positive values, the magnitude of the repulsive electrostatic interaction decreases while the pull-off force increases. At increasingly positive electrode potentials, the substrate obtains a net positive surface charge, which produces an attractive electrostatic interaction with the probe tip. This transition from repulsive to attractive electrostatic forces can be clearly seen (Figure 2b) along with an increase in the adhesive pull-off force at positive potentials. These results are consistent with previous measurements at gold and platinum electrodes, where a transition between repulsive and attractive electrostatic interactions is observed as the potential applied to these electrodes is moved from negative to positive values with respect to the potential of zero charge (E_{pzc}).[14,16] In the absence of specific adsorption or charge-transfer reactions, these differences in interaction forces between probe and substrate clearly reflect a change in the amount of electronically induced charge present on the electrode surface as the electrochemical potential is varied.

A comparison of these results to those obtained for a SPANi-coated electrode indicates a similar behavior. As illustrated in Figure 1b, positive excursions in the electrochemical potential applied to a SPANi film result in polymer oxidation. This transforms the polymer from its negatively charged, reduced state to an oxidized state that is nominally neutral or positively charged, depending upon the relative quantity of bound sulfonate and injected positive charge. Force measurements between SPANi and SiO_2 were performed in a solution with a pH of 2.5 (±0.5). Under these conditions, the SiO_2 probe is positive of its isoelectric point, so that it retains a small, negative surface

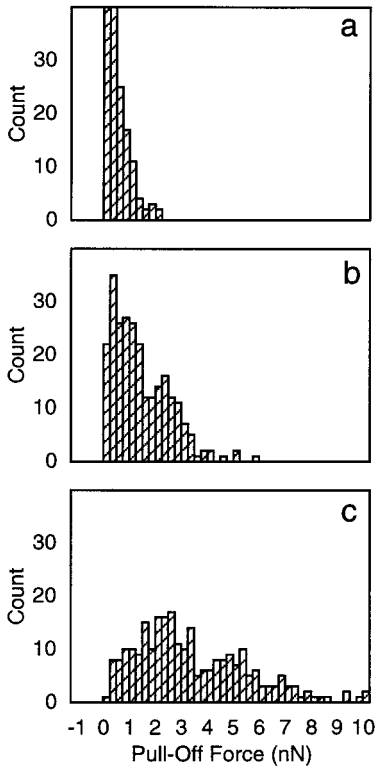

Figure 3. Representative pull-off force measurements between the SiO_2 tip and the SPANi substrate at substrate potential values of (a) −350 mV, (b) −50 mV, and (c) +150 mV (vs AgQRE). Each plot represents the results from 256 force curves, and the reported adhesive force at each potential is taken as the average value.

charge. At negative electrode potentials, the SPANi film possesses a negative charge dispersed throughout the film. Interaction between this negatively charged film and the negatively charged probe produces a repulsive force, which extends to a separation of approximately 20 nm from the surface (Figure 2c). Increasing the electrode potential toward more positive values initiates polymer oxidation. This oxidation is accompanied by a reduction in the repulsive force observed in the tip−sample interaction curve. The repulsive force continues to decrease as the electrode potential is increased toward more positive values. A net attractive force is observed when the potential reaches approximately −150 mV and becomes uniformly attractive at potentials greater than +100 mV (Figure 2d). Simultaneous with this decrease in repulsive interaction is an increase in the magnitude of the pull-off force. Thus, the variation in the shape of the force curves and the magnitude of the pull-off force track the electrochemical potential during SPANi oxidation in a manner that is identical to that seen for the simple double-layer charging of the carbon electrode.

Adhesive Forces. The picture of the carbon and SPANi interfaces obtained thus far suggests that the magnitude of the electrostatic force tracks the electrochemically induced charge present on the substrate surface. The nature of this transition can be further illustrated by considering the magnitude of the pull-off force between the tip and the substrate. Pull-off force values measured at three different electrode potentials for the SiO_2/SPANi interface exhibit a distribution of magnitudes (Figure 3). At negative electrode potentials (−350 mV), where the SPANi is in its fully reduced state, the pull-off force approaches an average value of 0.35 nN (Figure 3a). As the electrode potential is increased to more positive values (−150 mV and +50 mV), the distribution of measured

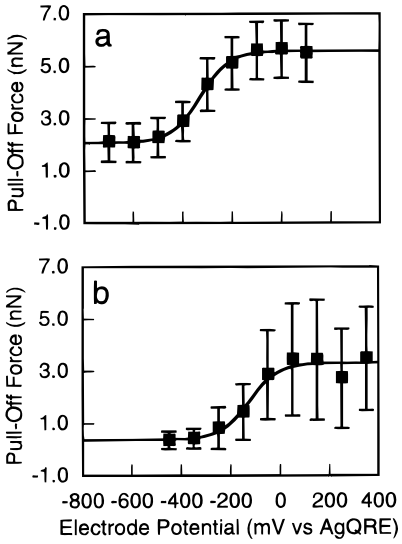

Figure 4. Summary of pull-off force measurements as a function of the electrochemical potential applied to the substrate. Pull-off force for (a) glassy carbon and (b) SPANi-coated electrodes. Each data point represents the average of 256 measurements, and the error bar is the standard deviation. The solid lines represent least squares fits to a titration curve. These curves give $E°$ values of −341 and −100 mV for plots a and b, respectively.

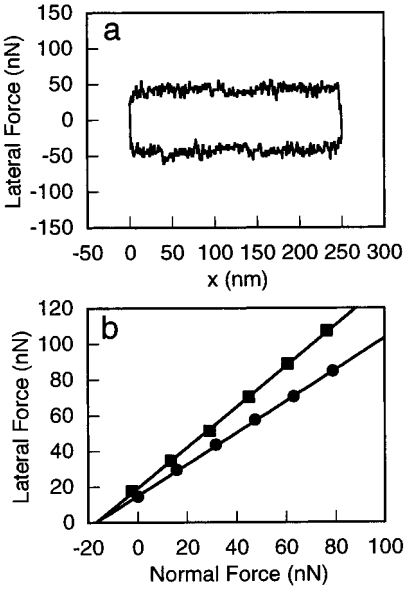

Figure 5. (a) Friction loop showing the trace and retrace of lateral force between the SiO_2 tip and the glassy carbon disk in 1 mM KCl at 25 °C and pH = 5.2 at an applied load of 28 nN and an applied electrochemical potential of +100 mV (vs SCE). (b) Plot of the lateral force versus the normal force at electrode potentials of (filled squares) +100 mV and (filled circles) −500 mV (vs AgQRE). The solid lines are best fits of the friction data to a straight line, with the slope giving the friction coefficient.

pull-off forces shifts toward more positive values (Figure 3b and c). This increase in pull-off force tracks the decrease in repulsive electrostatic interaction seen between the SiO_2 and SPANi surfaces. A similar increase in pull-off force is also observed between SiO_2 and carbon as the applied potential is increased toward more positive values.

The variation in pull-off force with electrode potential was tabulated for both carbon and SPANi surfaces. The pull-off force for the SiO_2/carbon interface shows a minimum value of 2 nN at negative electrode potentials, which increases to a maximum value of 5.5 nN at potentials positive of −200 mV (Figure 4a). The manner in which this transformation occurs can be readily fit to a titration-like curve, which exhibits saturation behavior at extreme positive and negative potentials and a transition region with a slope of approximately 60 mV/decade of force change. This resemblance to a titration curve is reasonable considering that this electrochemically induced charging process is equivalent to a change in ionization state of the surface. The minimum and maximum adhesion values reflect a surface that is saturated with either negative or positive charge.

A least squares curve fit of the titration curve for SiO_2/carbon identifies the data's inflection point at −341 mV. This inflection point should correspond to the potential where the electrostatic force transforms from repulsive to attractive and, thus, corresponds to the potential of zero charge E_{pzc}. Tabulation of the pull-off forces for the SiO_2/SPANi interface exhibits a similar titration-like response, with the inflection occurring at −125 mV (Figure 4b), which is approximately equal to the half-wave potential observed by cyclic voltammetry (Figure 1b). These observations of adhesive force variations with electrode potential are consistent with previous measurements of adhesive forces observed during electrochemical oxidation of an electroactive film.[21,22]

Friction Coefficient. Several recent studies using the surface forces apparatus[40] and atomic force microscope[30] have suggested a connection between adhesion and friction that derives from a common energy dissipation mechanism. Therefore, we suspected that the potential-dependent variation in adhesion observed in Figure 4 should be tracked by similar changes in friction. The friction coefficient is obtained by measuring the lateral force as a function of normal force. An example of a friction loop between SiO_2 and glassy carbon is shown in Figure 5a. The lateral force, which is calculated as the average of the forward and reverse traces, is determined for a given friction loop and then plotted as a function of increasing normal load force (Figure 5b). The friction coefficient is determined by assuming a linear relation between the lateral force F_L and the normal force F_N (eq 1)

$$F_L = F_0 + \mu F_N \tag{1}$$

where F_0 is a constant friction force arising from adhesion between the tip and the sample and μ is the normal friction coefficient.[40] The solid line through each set of points represents a best fit of the data to this equation. These data illustrate the change in friction coefficient for a glassy carbon surface at two different electrode potential values. The upper curve (solid squares, Figure 5b) was determined at an electrode potential of +100 mV while the lower curve (solid circles, Figure 5b) was determined at an electrode potential of −500 mV.

A series of friction coefficient values were determined for both glassy carbon and SPANi surfaces as the electrode potential was varied. The results for the SiO_2/carbon interface depict a response in which the friction coefficient possesses a small value at negative electrode potentials and increases with increasing potential values (Figure 6a). This response, when fit to a titration-like curve, gives an inflection point at −370 mV. When the response is plotted versus the measured pull-off force values, a straight line is obtained. This suggests that, indeed, the pull-off force and the friction coefficient for the SiO_2/carbon surface

(40) Yoshizawa, H.; Chen, Y.-L.; Israelachvili, J. *J. Phys. Chem.* **1993**, *97*, 4128−4140.

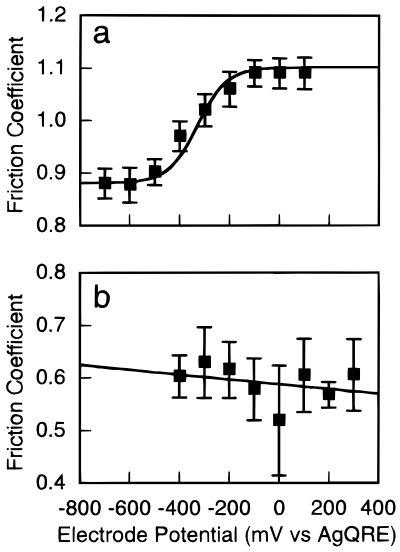

Figure 6. Measured friction coefficient as a function of applied electrochemical potential. Friction coefficient for (a) glassy carbon and (b) SPANi in 1 mM KCl solution at 25 °C and pH values of 5.2 and 2.5, respectively. The solid line in part a is a least squares fit to a titration curve with and $E°$ value of −370 mV. The solid line in part b is a least squares fit to a straight line. The points represent the average value, and the error bars are the standard deviation of values found for each electrochemical potential value.

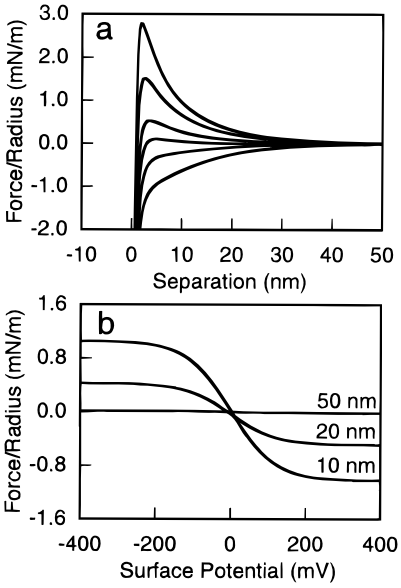

Figure 7. (a) Calculated force between a sphere and a plate for a fixed sphere potential as a function of plate potential in a 1 mM solution of 1:1 electrolyte from DLVO theory using a numerical solution to the nonlinear Poisson−Boltzmann equation with constant-charge boundary conditions and a nonretarded Hamaker constant of 1.0×10^{-20} J. The sphere potential is fixed at −41 mV while the plate potential varies from −100 mV (upper curve) to +100 mV (lower curve). (b) Calculated surface force between the tip and substrate as a function of the surface potential at tip−substrate separations of 50, 20, and 10 nm.

are correlated and are controlled by the variation in electrostatic force. These results are consistent with previous studies examining the variation in friction coefficient on platinum and metal oxide surfaces as a function of surface charge.[25,27]

In a similar manner, a series of friction coefficient values were measured between the SiO_2 probe and a SPANi-coated electrode as the electrode potential was changed from negative to positive values (Figure 6b). Results of these measurements indicate that the friction coefficient was relatively insensitive to the potential applied to the electrode surface and, consequently, the oxidation state of the SPANi film. In fact, within the error bars of the measurement, the friction coefficient remained constant as the substrate potential was varied. This is in contrast to the results seen for the SiO_2/carbon interface and, indeed, contrary to our expectations. Our measurements of electrostatic and pull-off forces clearly demonstrate a change from repulsive to attractive electrostatic interactions as the SPANi film is oxidized. However, these results are consistent with the apparent lack of variability seen in the friction coefficient of other modified electrode surfaces.[21] We hypothesize that this inconsistency in friction coefficient variation is a result of the contact geometry of the tip/sample interface, which is fundamentally different for the SiO_2/carbon and SiO_2/SPANi interfaces (vide infra).

Calculated Potential-Dependent Electrostatic Force. With the exception of the friction coefficient for SPANi, the observed variations in interfacial properties can be readily explained by considering the interactions between the tip and the sample as a function of substrate surface charge. The forces acting between electrostatic diffuse double layers can be described by the Derjaguin−Landau−Verwey−Overbeek (DLVO) theory.[41−44] The total interaction force (F_T) between two surfaces in an electrolyte solution, in the absence of solvent ordering or depletion forces, is thought to be comprised of the sum of an attractive van der Waals component (F_{vdW}) and an electrostatic repulsion or attraction (F_{dl}) due to the accumulation of charged ions in the gap.

$$F_T = F_{vdW} + F_{dl} \tag{2}$$

Using the Derjaguin approximation, the force between spheres of effective radius R_T can be related to the interaction energy W between plates by the expression

$$F_T = 2\pi R_T W_T = 2\pi R_T (W_{vdW} + W_{dl}) \tag{3}$$

where W_{vdW} and W_{dl} are the van der Waals and double-layer energies, respectively.

Using a previously described procedure,[16] a series of force curves were calculated using eq 3 (Figure 7a). In these curves, constant-charge boundary conditions were assumed with a fixed tip potential of −41 mV, substrate potentials varying from −100 to +100 mV, and a Hamaker constant of 1.0×10^{-20} J. These calculations demonstrate that when the probe and substrate possess potentials of opposite sign, the interaction force is purely attractive (lower curve). The long-range attraction is due to electrostatic interactions while the short-range attraction is van der Waals in nature. When the two surfaces have potentials of the same sign, the interaction is repulsive at large separations and becomes attractive as the surfaces approach (upper curve). This leads to a maximum in the force−distance curve that depicts the emergence of an attractive van der Waals component at close separations. Although constant-potential boundary conditions can also

(41) Derjaguin, B. *Trans. Faraday Soc.* **1940**, *36*, 203.
(42) Derjaguin, B. V.; Landau, L. D. *Acta Phys. Chem.* **1941**, *14*, 633.
(43) Derjaguin, B. V.; Landau, L. D. *J. Exp. Theor. Phys.* **1941**, *11*, 802.
(44) Verway, E. J.; Overbeek, J. T. G. *Theory of Lyophobic Colloids*; Elsevier: New York, 1948.

be employed, the constant-charge boundary conditions used here typically provide a more accurate representation of experimental data.[16] These simulated interaction curves qualitatively reflect the trends observed in the measured interaction forces between the SiO_2 tip and both carbon and SPANi interfaces.

Calculated Potential-Dependent Adhesion Force. The influence of electrochemical potential on the pull-off force or the adhesion force has been examined by several authors.[14,20] The results presented here clearly show a variation in pull-off force with electrode potential for both carbon and SPANi surfaces. This variation can be evaluated by considering the various interactions at the tip/substrate interface during contact. The forces observed during approach are described primarily by "noncontact" interactions such as van der Waals and double-layer forces. However, following contact, tip−sample bonding produces an additional adhesive force that must be overcome to separate these surfaces. According to the JKR theory of contact mechanics,[45] the force required to separate a sphere and a flat surface ($F_{\text{pull-off}}$) is related to the work of adhesion (W_{adh})

$$F_{\text{pull-off}} = -^3/_2 \pi R_T W_{\text{adh}} \quad (4)$$

The work of adhesion can be related to the surface free energies of the various system interfaces

$$W_{\text{adh}} = \gamma_{\text{tip/solvent}} + \gamma_{\text{substrate/solvent}} - \gamma_{\text{tip/substrate}} \quad (5)$$

where $\gamma_{\text{tip/solvent}}$ and $\gamma_{\text{substrate/solvent}}$ represent the tip/solvent and substrate/solvent interfaces while $\gamma_{\text{tip/substrate}}$ is the free energy associated with tip/substrate interface. The work of adhesion can also be considered as the sum of terms associated with tip−substrate bonding (W_{bond}), van der Waals interactions (W_{vdW}), and the energy associated with the formation of a double layer (W_{dl}).

$$W_{\text{adh}} = W_{\text{bond}} + W_{\text{vdW}} + W_{\text{dl}} \quad (6)$$

As illustrated by the experimental data, a titration-like response was observed in the magnitude of the pull-off force for both carbon and SPANi surfaces as the electrode potential was changed from negative to positive values. A comparison to the theoretical predictions demonstrates that the calculated electrostatic force (F_{dl}), which is equivalent to the free energy of the double layer (W_{dl}), follows a similar trend (Figure 7b). A plot of the calculated interaction force at several different separations as the surface potential is varied shows that when the tip and the substrate are of similar charge, the surface forces are repulsive and saturate to a constant value. As the surface potential of the substrate is increased to more positive values, the repulsive force gradually decreases until, at extreme positive potentials, the interaction again saturates to a constant negative or attractive value. This saturation-like behavior can be most readily explained in terms of the saturation in surface charge that occurs at high and low surface potentials

Equation 6 clearly indicates that, when the tip/sample bonding and van der Waals interaction terms are constant, changes in the electrostatic interaction (W_{dl}) will be the primary source for measured differences in W_{adh} and, consequently, $F_{\text{pull-off}}$. Thus the variation in pull-off force with electrode potential for the SiO_2/carbon interface is simply a reflection of the change in W_{dl} from repulsive values, giving a smaller magnitude for W_{adh}, compared to attractive values, where W_{adh} is a maximum. Indeed, the observation of similar potential-dependent behavior for the SiO_2/SPANi interface also suggests that the transformation in pull-off force is dominated by the electrostatic component.

Scheme 1. Schematic of the Interfacial Contact Region and the Interaction Forces Acting between a Charged Tip and Rigid Substrate in an Electrolyte Solution

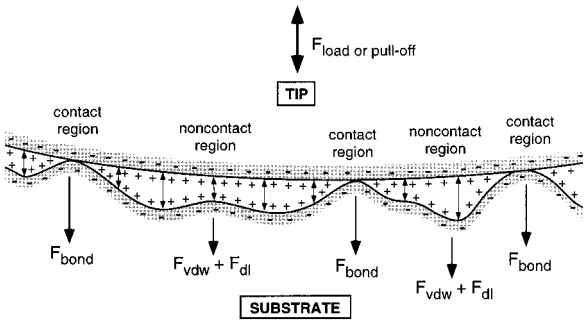

This observation is significant when we consider the ability to accurately determine tip−sample adhesive bonding in liquid environments in the presence of electrolyte solution. To eliminate the influence of electrostatic effects, the pull-off force and tip−substrate adhesion can only be equated at the potential of zero charge, which occurs at the inflection point in the pull-off force versus potential curves (Figure 4). On the basis of the measured values, the tip−substrate adhesion force is approximately 4.2 nN for SiO_2/carbon and 1.8 nN for SiO_2/SPANi.

Calculated Potential-Dependent Friction Coefficient. The observation of potential-dependent frictional variations for the SiO_2/carbon interface contrasts those values measured for the SiO_2/SPANi interface, which exhibits nearly constant friction coefficient values. A proposed explanation for this behavior focuses on the geometry of the interfacial contact region between the probe and substrate. For an atomically smooth interface, the tip−sample contact area should be equal to the geometric area of contact. However, since most surfaces exhibit at least some degree of microscopic roughness, the actual contact area (A_0) will be somewhat less than the geometric area (A). As shown in Scheme 1, surface roughness leads to the formation of numerous microcontacts at the tip/substrate interface.[25,27] This structure must be taken into account when considering the friction coefficient. The definition of the friction coefficient is given as the ratio of the lateral force (F_L) to the normal force (F_N)

$$\mu = F_L/F_N \quad (7)$$

The lateral force can be equated to the yield strength of the weaker of the two materials (σ_T) times the contact area (A_0)

$$F_L = \sigma_T A_0 \quad (8)$$

The normal force must include the interactions at both contact and noncontact regions of the interface. The tip−substrate bonding interaction (F_{bond}) and load force (F_{load}) both operate through the adhesive contact regions represented by the micro-contacts with an area A_0. In Scheme 1, the regions between contacts possess voids where the surfaces are not touching and contain some quantity of electrolyte. The tip−sample interaction in these void regions is dominated by noncovalent forces ($F_{\text{vdW}} + F_{\text{dl}}$),

(45) Johnson, K. L.; Kendall, K.; Roberts, A. D. *Proc. R. Soc. London, Ser. A* **1971**, *324*, 301.

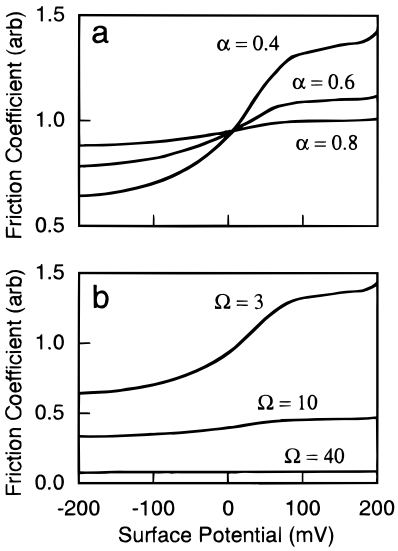

Figure 8. Calculated friction coefficient as a function of substrate surface potential as determined with eq 10. (a) Friction coefficient variation with electrode potential as a function of relative contact area for values of $\alpha = 0.4$, 0.6, and 0.8. (b) Friction coefficient variation with electrode potential as a function of applied load for ratios of applied load to DLVO force ($\Omega = F_{load}/(F_{vdW} + F_{dl})$) of $\Omega = 3$, 10, and 40. The DLVO force was evaluated for a tip−sample separation of 9.8 nm, and the adhesion force was taken as 4.2 nN. The yield strength was adjusted to give a friction coefficient near 1.

which we have previously described using DLVO theory. These DLVO interactions could be considered as functioning over an average separation distance that is proportional to the average surface roughness of the tip and the sample. Thus, in this system, the normal force is a function of the applied load (F_{load}), adhesive tip/substrate bonding interactions (F_{bond}), and noncontact DLVO forces. This normal force is then

$$F_N = [(A - A_0)(F_{vdW} + F_{dl}) + A_0(F_{bond} + F_{load})]/A \quad (9)$$

where A_0 is the contact area and $A-A_0$ is the gap region. The friction coefficient can now be considered as the ratio of the lateral force to the normal force

$$\mu = \sigma_T A_0/[(1 - \alpha)(F_{vdW} + F_{dl}) + \alpha(F_{bond} + F_{load})] \quad (10)$$

where α is the ratio of the contact area to the geometric interfacial area ($\alpha = A_0/A$), which varies between values of 0 and 1.

The two components of eq 10 that can have an impact on the friction coefficient in addition to the forces considered earlier are the contact area ratio (α) and the applied load. This load dependence will be considered as the ratio of the applied load to the DLVO forces (Ω),

$$\Omega = F_{load}/(F_{vdW} + F_{dl}) \quad (11)$$

It is instructive to plot the variation in relative friction coefficient with changing electrostatic force as a function of α and Ω. The change in friction coefficient with surface potential follows a titration-like response when the relative contact area is small in comparison to the total geometric area (Figure 8a). Under these conditions, a large percentage of the interfacial region corresponds to the microgap regions (Scheme 1), which are dominated by noncontact forces. However, as the contact area increases and α approaches a value of 1, the adhesive force dominates and the friction coefficient begins to be independent of surface

Scheme 2. Schematic of the Interfacial Contact Region and the Interaction Forces Acting between a Charged Tip and Compliant Substrate in an Electrolyte Solution

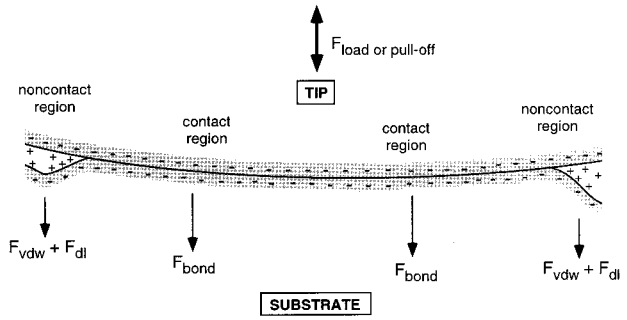

charge. Under these conditions, a majority of the interfacial area between the tip and substrate would be in contact (Scheme 2). For surfaces of similar surface roughness, this relative contact area must be a function of the elastic constants of the tip and the substrate, with α increasing in value for more compliant materials. In the systems examined here, SPANi is clearly softer or more compliant than glassy carbon. Therefore, the interfacial region between the SiO_2 probe and the carbon substrate likely has a smaller relative contact area, as in Scheme 1, while the SiO_2/SPANi interface will be dominated by adhesive contact due to the compressibility of the SPANi surface, as in Scheme 2. In this latter case, the solvent and electrolyte will be squeezed out of the tip−substrate gap and simultaneously reduce the effect of electrostatic forces.

Figure 8b suggests that the applied load will also have an impact upon the measured friction coefficient. As the ratio of the applied load to the DLVO forces increases, the measured friction coefficient will decrease and the potential dependence of the friction coefficient will disappear. However, these load-induced changes are not likely to be a factor in the measurements presented here due to the low load conditions used. In addition, this load effect would appear during measurements of the friction coefficient by a reduction in the friction coefficient with increasing applied load and the presence of nonlinearity in the frictional loading curves (Figure 5b). This behavior is not observed for carbon or SPANi surfaces.

A final comment concerning the lack of a frictional dependence on electrode potential for the SPANi-coated electrode is that this result must also serve as evidence for the absence of changes in the magnitude of tip−sample bonding during oxidation of the SPANi film. If one considers that the compliant interface in Scheme 2, which represents the SiO_2/SPANi interface, is dominated by the tip−substrate bonding force, then any change in that term would appear as a very strong deviation in friction as the potential is varied. These changes were not observed. Therefore, the simultaneous measurement of surface force, adhesion, and friction provides a potential method for evaluating changes in adhesive forces that can be clearly distinguished from electrostatic effects.

Conclusions

We have shown that the atomic force microscope can be used to simultaneously measure interfacial forces, adhesion, and the friction coefficient at the electrode/electrolyte interface. In the absence of potential-dependent compositional changes in the tip or the substrate, variations in surface charge are solely responsible for the observed changes in interfacial properties. Variations in electro-

static force, adhesion, and friction coefficient can all be fit to simple titration-like curves. DLVO theory can be used to describe these changes by considering the role of surface charge on the resulting normal tip−sample interaction forces. The observation of a charge-dependent friction coefficient between rigid surfaces is the result of electrolyte present within microgaps that exist between the tip and the substrate and the resulting formation of a diffuse double layer that contributes to the interfacial force. However, friction measurements between a rigid tip and a compliant SPANi film are insensitive to electrode potential while electrostatic and adhesion forces remain sensitive to surface charge. This result can be explained by considering the increased contact area between the tip and substrate for this compliant interface, which minimizes microgaps and eliminates electrolyte-containing solvent from the tip/sample interface. Thus, electrostatic forces do not operate between the tip and substrate during contact and the friction coefficient is, therefore, constant. Pull-off force measurements show a potential dependence for both rigid and compliant substrates because double-layer formation must contribute to the work of adhesion, regardless of the contact geometry.

Acknowledgment. Support of this research by the Camille and Henry Dreyfus Foundation through a New Faculty Award is gratefully acknowledged. We also wish to thank Molecular Imaging Corporation for a Young Electrochemical Scanning Probe Microscopist Award. We thank K. Andy Young for synthesis of the SPANi films.

LA981137U